VERTICAL MIXING PROCESSES IN STRATIFIED LAKES AND RESERVOIRS

CI 71Q HIDRODINAMICA AMBIENTAL Profs. Y. Niño & A. Tamburrino
Sem. Otoño 2004

Consider a stratified water body such as that shown in Fig. 1, with a surface layer of constant temperature and density, T_1 and ρ_1, respectively, (the epilimnion) and a bottom layer of constant temperature and density, T_2 and ρ_2, respectively, (the hypolimnion). The free surface is located at an elevation z_s measured with respect to the bottom of the water basin. Consider that the metalimnion, the region of large density and temperature gradients in between the surface and bottom layers, is rather narrow and located at an elevation z_T with respect to the bottom.

Vertical mixing in this system implies increasing the density of the upper layer, which is caused by an upwards mass flux of hypolimnetic water created by the deepening of the metalimnion region. Two different vertical mixing processes are considered in the following analysis: *Penetrative Convection* and *Wind Mixing*.

1 Penetrative Convection

During cooling phases, heat is released from the water body to the atmosphere. This tends to decrease the potential energy of the water body due to the shrinkage of the epilimnetic volume. The release of potential energy is transformed into turbulent kinetic energy that creates mixing within the metalimnion region. This occurs in the form of thermals that sink throughout the epilimnion, due to excess weight, and erode the metalimnion. In fact, as heat is released from the surface, colder and heavier water lays on top of the lighter and warmer water of the epilimnion. Thermals are created due to the instability of this surface cold layer.

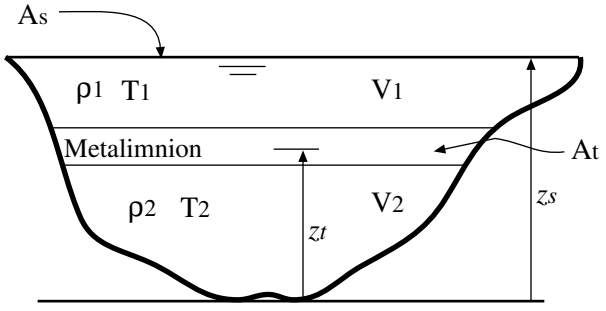

Figure 1: Stratified water basin.

1.1 Heat balance

To analyze mixing due to penetrative convection, it is convenient to start by establishing heat and mass balances within the system. Consider the release of some amount of heat to the atmosphere due to cooling effects. This occurs, for example, when the temperature of the water body is in excess of the equilibrium temperature. Call H_0 the heat flux released to the atmosphere. The heat balance within the epilimnion reads:

$$\rho_1 \, C_p \, V_1 \, \frac{dT_1}{dt} = -H_0 \, A_s - \rho_1 \, C_p \, \Delta T \, A_t \, u_e \tag{1}$$

where C_p denotes the specific heat of the water, V_1 is the volume of the epilimnion, t denotes time, A_s and A_t denote cross sectional areas at the free surface and at the elevation of the metalimnion, respectively, $\Delta T = T_1 - T_2$ denotes the temperature difference between the epilimnion and the hypolimnion and u_e represents the rate of deepening of the metalimnion due to mixing associated with the thermal erosion process. The latter is also known as *entrainment velocity*. The first term of the right hand side represents the heat released to the atmosphere through the free surface. The second term of the right hand side represents the amount of heat taken from the epilimnion to warm up water from the hypolimnion that is being mixed with that of the epilimnion due to the erosion of the metalimnion.

Equation (1) can be rewritten as:

$$\frac{dT_1}{dt} = -\frac{H_0}{\rho_1 \, C_p \, h_1} - \frac{A_t}{A_s} \, \frac{\Delta T}{h_1} \, u_e \tag{2}$$

where $h_1 = V_1/A_s$ denotes the mean height of the epilimnion.

Heat balance within the hypolimnion leads to the condition:

$$\frac{dT_2}{dt} = 0 \tag{3}$$

when heat transfer with the bottom of the water basin is neglected.

Invoking the linearized equation of state of water density:

$$\rho = \rho_0 \, (1 - \alpha \, T) \tag{4}$$

where ρ_0 is a reference density, T represents temperature and α is a contraction coefficient. From this equation it is concluded that:

$$\frac{d\rho_1}{dt} = -\alpha \, \rho_0 \, \frac{dT_1}{dt} \quad ; \quad \frac{d\rho_2}{dt} = -\alpha \, \rho_0 \, \frac{dT_2}{dt} \quad ; \quad \Delta\rho = \rho_2 - \rho_1 = \alpha \, \rho_0 \, \Delta T \tag{5}$$

Replacing (5) in (2) and (3) yields:

$$\frac{d\rho_1}{dt} = \alpha \, \rho_0 \, \frac{H_0}{\rho_1 \, C_p \, h_1} + \frac{A_t}{A_s} \, \frac{\Delta\rho}{h_1} \, u_e \tag{6}$$

$$\frac{d\rho_2}{dt} = 0 \tag{7}$$

Both the temperature and density of the hypolimnion are conserved during the mixing process.

1.2 Mass balance

Consider now mass balance in both epilimnion and hypolimnion.

$$\frac{d(\rho_1\ V_1)}{dt} = \rho_2\ A_t\ u_e \tag{8}$$

$$\frac{d(\rho_2\ V_2)}{dt} = -\rho_2\ A_t\ u_e \tag{9}$$

which obviously indicate that the total mass of the system $(\rho_1\ V_1 + \rho_2\ V_2)$ is conserved.

Since $d\rho_2/dt = 0$, then:

$$\frac{dV_2}{dt} = -A_t\ u_e \tag{10}$$

Expanding (8) yields:

$$V_1\ \frac{d\rho_1}{dt} + \rho_1\ \frac{dV_1}{dt} = \rho_2\ A_t\ u_e \tag{11}$$

or, since $V_1 = A_s\ h_1$:

$$h_1\ \frac{d\rho_1}{dt} + \rho_1\ \frac{dh_1}{dt} = \rho_2\ \frac{A_t}{A_s}\ u_e \tag{12}$$

and using (6):

$$\frac{dh_1}{dt} = \frac{A_t}{A_s}\ u_e - \alpha\ \frac{\rho_0}{\rho_1}\ \frac{H_0}{\rho_1\ C_p} \tag{13}$$

1.3 Closure for the entrainment velocity

To predict the temperature and volume changes in the epilimnion due to penetrative convection a closure for the entrainment velocity is needed. For that, an energy balance is to be considered next.

Potential energy change due to cooling

As heat is released from the epilimnion, its temperature decreases as predicted by (2). This has the effect of lowering the center of mass of the water body as a whole, due to the contraction of the water volume, and of decreasing the potential energy of the system. Part of the released potential energy goes to the kinetic energy associated with the thermals, which is then used to erode the metalimnion.

The potential energy of the water basin is given by:

$$P = \int_0^{z_T}\ \rho_2\ g\ z\ A(z)\ dz + \int_{z_T}^{z_s}\ \rho_1\ g\ z\ A(z)\ dz \tag{14}$$

where $A(z)$ denotes the cross sectional area of the water basin at an elevation z. Assuming that ρ_1 and ρ_2 are constant within the respective surface and bottom layers and that $d\rho_2/dt = 0$ according to (7), the rate of change of the potential energy is then:

$$\frac{dP}{dt} = g\ \{\rho_2\ z_T\ A_t\ \frac{dz_T}{dt} + \frac{d\rho_1}{dt}\ \int_{z_T}^{z_s}\ z\ A\ dz + \rho_1\ z_s\ A_s\ \frac{dz_s}{dt} - \rho_1\ z_T\ A_t\ \frac{dz_T}{dt}\} \tag{15}$$

Using (10), z_T is defined such that $V_2 = z_T\ A_t$ and:

$$\frac{dz_T}{dt} = -u_e \tag{16}$$

Besides, $V_1 = \int_{z_T}^{z_s}\ A\ dz$, therefore:

$$\frac{dV_1}{dt} = A_s\ \frac{dz_s}{dt} - A_t\ \frac{dz_T}{dt} = A_s\ \frac{dz_s}{dt} + A_t\ u_e \tag{17}$$

and:

$$z_{v1} = \frac{1}{V_1}\ \int_{z_T}^{z_s}\ z\ A\ dz \tag{18}$$

denotes the center of volume of the epilimnion.

Replacing (6), (13), (16), (17) and (18) in (15) yields the rate of change of the potential energy as:

$$\frac{dP}{dt} = g\ \Delta\rho\ A_t\ (z_{v1} - z_T)\ u_e - \alpha\ \rho_0\ g\ A_s\ \frac{H_0}{\rho_1\ C_p}\ (z_s - z_{v1}) \tag{19}$$

which represents a balance between the gain in potential energy due to mixing (first term in the right hand side) and the decrease of potential energy due to the release of heat from the surface water to the atmosphere (second term in the right hand side). Obviously, if penetrative convection is to create mixing through the development of thermals, the second term is more important than the first one and the potential energy decreases as a consequence of cooling.

Equation (19) can be rewritten in terms of the temperature difference ΔT instead of the density difference $\Delta\rho$:

$$\frac{dP}{dt} = \alpha\ \rho_0\ g\ \Delta T\ A_t\ (z_{v1} - z_T)\ u_e - \alpha\ \rho_0\ g\ A_s\ \frac{H_0}{\rho_1\ C_p}\ (z_s - z_{v1}) \tag{20}$$

Kinetic energy of the thermals

The potential energy released due to cooling is partially used to increase the kinetic energy of the thermals that erode the metalimnion. The energy balance can be expressed as (Fisher et al., 1979):

$$\frac{dK}{dt} = -\frac{dP}{dt} - \Phi \tag{21}$$

where K denotes the kinetic energy of the thermals and Φ denotes rate of viscous dissipation of energy within the system.

A bulk estimate of K is proposed by Fisher et al. (1979) as:

$$K = \frac{1}{2}\ c_t\ \rho_1\ V_1\ u_t^2 \tag{22}$$

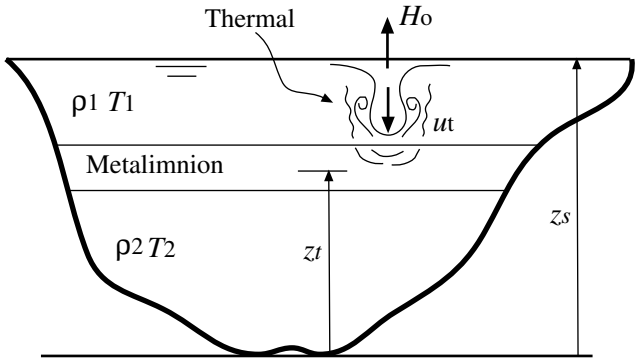

Figure 2: Thermal eroding the metalimnion.

where c_t is a coefficient and u_t represent the fall velocity of the thermals (Fig. 2).

To estimate u_t another energy balance can be considered. Near the surface the energy of the colder water that will form the thermal is proportional to $g' z_s$, where $g' = g\ (\Delta\rho)_t/\rho_1$ is the reduced gravity affecting the thermals, where $(\Delta\rho)_t$ represents the density difference between the colder water in the thermal and the warmer water of the epilimnion. Near the metalimnion, where mixing takes place, the energy of the thermal is proportional to $g' z_T + u_t^2/2$. Therefore, with reference to Fig. 2:

$$m\ g'\ z_s = m\ g'\ z_T + m\ \frac{u_t^2}{2} \tag{23}$$

where m denotes the mass of a fluid parcel that falls within the thermal. Hence:

$$u_t^2 = 2\ g'\ (z_s - z_T) = 2\ g\ \frac{(\Delta\rho)_t}{\rho_1}\ (z_s - z_T) \tag{24}$$

From (4), the density difference in the thermal can be expressed in terms of temperature difference between the thermal and the epilimnetic water:

$$(\Delta\rho)_t = \alpha\ \rho_0\ (\Delta T)_t \tag{25}$$

This temperature difference can be estimated in terms of the equilibrium between the heat flux extracted by the thermal from the epilimnion and the heat flux released to the atmosphere:

$$\rho_1\ C_p\ (\Delta T)_t\ u_t = H_0 \tag{26}$$

from where the temperature difference of the thermal results to be:

$$(\Delta T)_t = \frac{H_0}{\rho_1\ C_p\ u_t} \tag{27}$$

Replacing (27) in (24) leads to:

$$u_t = \{2\ \alpha\ \frac{\rho_0}{\rho_1}\ \frac{H_0}{\rho_1\ C_p}\ g\ (z_s - z_T)\}^{1/3} \tag{28}$$

Using the same arguments Fisher et al. (1979) propose the following equation for u_t, which is slightly different to (28):

$$u_t = \{\alpha\ g\ \frac{H_0}{\rho_1\ C_p}\ (z_s - z_T)\}^{1/3} \tag{29}$$

Entrainment velocity

The rate of change of the kinetic energy of the thermals is given from (22) as:

$$\frac{dK}{dt} = \frac{1}{2}\ c_t\ \frac{d(\rho_1\ V_1)}{dt}\ u_t^2 = \frac{1}{2}\ c_t\ \rho_2\ u_e\ A_t\ u_t^2 \tag{30}$$

Replacing this result in (21) yields:

$$\frac{1}{2}\ c_t\ \rho_2\ u_e\ A_t\ u_t^2 = -\alpha\ \rho_0\ g\ \Delta T\ A_t\ (z_{v1} - z_T)\ u_e + \alpha\ \rho_0\ g\ A_s\ \frac{H_0}{\rho_1\ C_p}\ (z_s - z_{v1}) - \Phi \tag{31}$$

and since:

$$\frac{H_0}{\rho_1\ C_p} = \frac{u_t^3}{\alpha\ g\ (z_s - z_T)} \tag{32}$$

the following expression is obtained:

$$\{c_t\ u_t^2 + \alpha\ g\ \Delta T\ 2\ (z_{v1} - z_T)\}\ u_e = u_t^3\ \{2\ \frac{z_s - z_{v1}}{z_s - z_T}\ \frac{A_s}{A_t} - \frac{2\ \Phi}{\rho_0\ A_t\ u_t^3}\} \tag{33}$$

It is easy to see that the first term inside the parenthesis of the right hand side is of order one. Fisher et al. (1979) argue that the second term inside the parenthesis of the right hand side can be approximated as a constant coefficient. They propose the following approximation:

$$2\ \frac{z_s - z_{v1}}{z_s - z_T}\ \frac{A_s}{A_t} - \frac{2\ \Phi}{\rho_0\ A_t\ u_t^3} \approx 1 - \frac{2\ \Phi}{\rho_0\ A_t\ u_t^3} = c_k \tag{34}$$

where c_k is a constant coefficient. Equation (33) can then be rearranged as:

$$\frac{u_e}{u_t} = c_k\ \{c_t + \frac{\alpha\ g\ \Delta T}{u_t^2}\ 2\ (z_{v1} - z_T)\}^{-1} \tag{35}$$

Now rewrite the dimensionless term in the right hand side:

$$\frac{\alpha\ g\ \Delta T}{u_t^2}\ 2\ (z_{v1} - z_T) = g\ \frac{\Delta\rho}{\rho_0}\ \frac{2\ (z_{v1} - z_T)}{u_t^2} = \frac{g'\ h}{u_t^2} = \frac{1}{Fr_d^2} = Ri \tag{36}$$

where $g' = g\ \Delta\rho/\rho_0 = g\ (\rho_2 - \rho_1)/\rho_0$ denotes the reduced gravity of the stratified water body and $h = 2\ (z_{v1} - z_T)$ is a length scale representing the thickness of the epilimnion. In this equation Fr_d represents a *Densimetric Froude Number* and Ri is the corresponding *Richardson Number*.

From (35), the dimensionless entrainment velocity is finally given by:

$$\frac{u_e}{u_t} = \frac{c_k}{(c_t + Ri)} \tag{37}$$

which predicts that the dimensionless entrainment velocity increases as the Richardson number decreases, that is, as the heat released to the atmosphere, H_0, increases. On the contrary, when H_0 vanishes, Ri goes to infinity and the entrainment velocity vanishes. Based on field measurements, Fisher et al. (1979) propose the values $c_k = 0.13$ and $c_t = 0.5$.

Pedersen (1986) argues that c_k represents actually a *Bulk Flux Richardson Number*. Its value should be in a rather narrow range: $0.04 < c_w < 0.18$, with the upper limit corresponding to mixing processes associated to the phenomenon of vortex formation and pairing at the interface and the lower limit corresponding to entrainment caused by internal wave breaking mechanisms. According to Pedersen a proper value of c_k for entrainment by penetrative convection would be the upper limit, $c_k = 0.18$.

2 Wind Mixing

Consider now that the surface layer is at the equilibrium temperature so that the heat exchange with the atmosphere is negligible, but there is wind blowing over the free surface. In this case, it is the momentum transfer by the wind what is relevant in terms of the vertical mixing processes in the system. The input of momentum by the wind creates turbulent kinetic energy in the surface water which is diffused down towards the metalimnion. Turbulent mixing within this region increases the potential energy of the water body, as its center of mass is displaced upwards due to the increased density (and reduced temperature) of the epilimnion resulting from the mixing with colder and heavier water from the hypolimnion.

2.1 Heat balance

Since in this problem heat exchange with both the atmosphere and the bottom of the water body can be neglected, the heat balance expressed by the already deduced equations (2) and (3) reduces to:

$$\frac{dT_1}{dt} = -\frac{A_t}{A_s}\,\frac{\Delta T}{h_1}\,u_e \tag{38}$$

$$\frac{dT_2}{dt} = 0 \tag{39}$$

which predict that the temperature of the hypolimnion remains constant, while that of the epilimnion decreases as wind mixing proceeds. Here, u_e denotes the entrainment velocity associated to the latter process.

In terms of density variations, these equations are expressed as:

$$\frac{d\rho_1}{dt} = \frac{A_t}{A_s}\,\frac{\Delta \rho}{h_1}\,u_e \tag{40}$$

$$\frac{d\rho_2}{dt} = 0 \tag{41}$$

which indicate that as the temperature of the epilimnion decreases its density increases, while that of the hypolimnion remains constant.

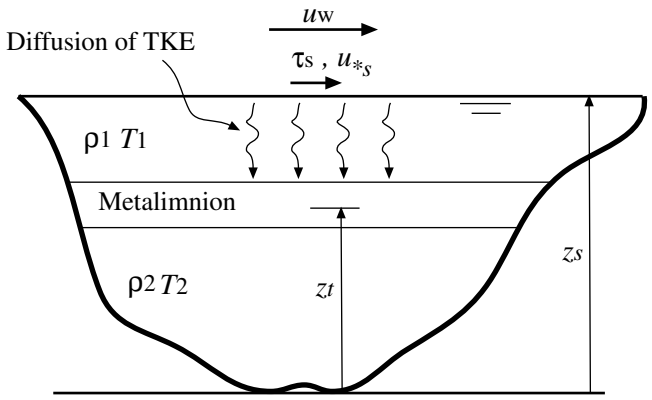

Figure 3: Wind mixing by diffusion of turbulent kinetic energy (TKE) within the epilimnion.

2.2 Mass balance

Just as in the case of penetrative convection, the mass balance is expressed by:

$$\frac{d(\rho_1 V_1)}{dt} = \rho_2 A_t u_e \tag{42}$$

$$\frac{d(\rho_2 V_2)}{dt} = -\rho_2 A_t u_e \tag{43}$$

which indicate that the total mass of the system $(\rho_1 V_1 + \rho_2 V_2)$ is conserved.

Replacing (40) in (42) and (41) in (43) gives:

$$\frac{dh_1}{dt} = \frac{A_t}{A_s} u_e \tag{44}$$

$$\frac{dz_T}{dt} = -u_e \tag{45}$$

where $h_1 = V_1/A_s$ and $z_T = V_2/A_t$. These two equations are just two equivalent ways to understand the rate of deepening of the density interface due to wind mixing. Changes in h_1 are only generated by the mixing process and there are no volume changes associated to heat exchange with the atmosphere involved as in the previous case analyzed.

2.3 Closure for the entrainment velocity

A closure for the entrainment velocity associated with wind mixing requires a different energy balance with respect to that used in the analysis of penetrative convection. In this case the turbulent kinetic energy input at the free surface is diffused down towards the metalimnion (Fig. 3). The rate at which this energy becomes available for mixing dictates the rate at which the potential energy of the water body increases due to mixing.

Potential energy increase due to mixing

Using the result given by (20) and imposing a vanishing heat flux exchange with the atmosphere, $H_0 = 0$, yields:

$$\frac{dP}{dt} = g\ \Delta\rho\ A_t\ (z_{v1} - z_T)\ u_e \tag{46}$$

which indicates that the rate at which the potential energy of the water body increases is proportional to the entrainment velocity.

The rate of change of P is dictated by the rate of change of the turbulent kinetic energy available for mixing in the metalimnion:

$$\frac{dP}{dt} = \frac{dK}{dt} \tag{47}$$

where the right hand side represents the rate at which turbulent kinetic energy is made available for the mixing process.

Diffusion of turbulent kinetic energy in the epilimnion

Turbulent kinetic energy, K, is transferred by the wind to the surface water and then diffused down to the metalimnion. A transport equation for K within the epilimnion can be simply expressed as:

$$\frac{\partial K}{\partial t} = -\frac{\partial(\overline{w'K'})}{\partial z} - \Phi \tag{48}$$

where $\overline{w'K'}$ represents the vertical flux of turbulent kinetic energy associated with turbulent diffusion and Φ is a bulk rate of viscous dissipation. In this equation, production of turbulent kinetic energy within the epilimnion is neglected for simplicity, however this term may be an important contribution to the energy balance if high velocity gradients are present in the surface region associated with drift currents induced by the wind.

To model the diffusion term, the following approximation is introduced:

$$-\frac{\partial(\overline{w'K'})}{\partial z} \simeq \frac{w'\ K}{h_1} \tag{49}$$

where w' is a velocity scale representing the vertical component of the RMS of the turbulent velocity fluctuations within the epilimnion, K is an estimation of the turbulent kinetic energy content in the epilimnion and $h_1 = V_1/A_s$ is a measure of the epilimnion height.

A value of K can be estimated as:

$$K \propto \frac{3}{2}\ (\rho_1\ V_1)\ (w')^2 \tag{50}$$

On the other hand, w' can be modelled by assuming that it scales with the surface shear velocity induced by the wind, $u_{*s}^2 = \tau_s/\rho_1$, where τ_s denotes the wind induced surface shear stress. This quantity is usually estimated as a function of the wind speed as:

$$\tau_s = \rho_a\ C_{Dw}\ u_w^2 \tag{51}$$

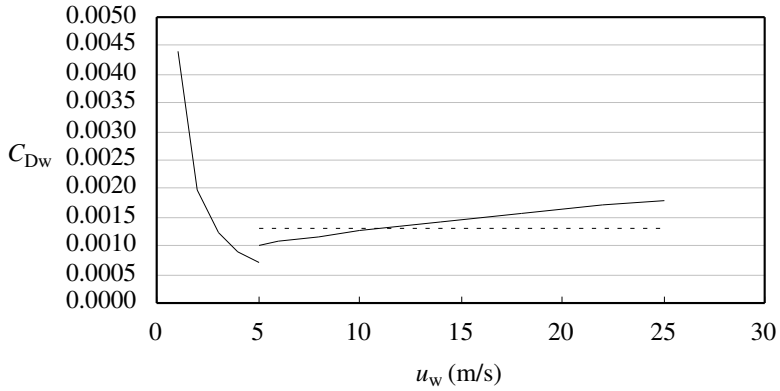

Figure 4: Wind drag coefficient as a function of wind velocity (after Wüest and Lorke, 2003). The expressions for the curves plotted with solid lines are: $C_{Dw} = 0.0044\ u_w^{-1.15}$ for $u_w < 5m/s$; and $C_{Dw} = (1/\kappa\ \ln(g\ 10/C_{Dw}/u_w^2) + 11.3)^{-2}$ for $u_w > 5m/s$, where κ denotes von Karman's constant. The dashed line represents $C_{Dw} = 0.0013$.

where ρ_a denotes the density of air (approximately equal to 1.2 kg/m^3), C_{Dw} is a wind drag coefficient, and u_w denotes the wind speed. A typical value of $C_{Dw} = 0.0013$ is used when u_w represents the wind speed at a reference height of 10 m above the free surface, which is valid when $u_w > 5m/s$. For lower values of the wind speed, C_{Dw} tend to increase as u_w decreases (Fig. 4).

With this assumptions the diffusion term in (48) is estimated as:

$$-\frac{\partial(\overline{w'K'})}{\partial z} = c_w\ \frac{3}{2}\ \rho_1\ A_s\ u_*^3 \tag{52}$$

where c_w is a coefficient. The rate at which turbulent kinetic energy is made available for mixing at the metalimnion is then:

$$\frac{dK}{dt} = c_w\ \frac{3}{2}\ \rho_1\ A_s\ u_*^3 - \Phi \tag{53}$$

Entrainment velocity due to wind mixing

Replacing this result in (47) and using (46) yields:

$$g\ \Delta\rho\ A_t\ (z_{v1} - z_T)\ u_e = c_w\ \frac{3}{2}\ \rho_1\ A_s\ u_*^3 - \Phi \tag{54}$$

or rearranging terms:

$$\{\frac{\Delta\rho}{\rho_0}\ g\frac{2\ (z_{v1} - z_T)}{u_{*s}^2}\}\ \frac{u_e}{u_{*s}} = 3c_w\ \frac{\rho_1}{\rho_0}\ \frac{A_s}{A_t} - \frac{2\ \Phi}{\rho_0\ A_t\ u_{*s}^3} \tag{55}$$

The dimensionless term in brackets in the left hand side can be written as:

$$\frac{\Delta\rho}{\rho_0}\ g\frac{2\ (z_{v1} - z_T)}{u_{*s}^2} = \frac{g'h}{u_{*s}^2} = Ri \tag{56}$$

where $g' = g\ \Delta\rho/\rho_0$ denotes reduced gravity, $h = 2\ (z_{v1} - z_T)$ is a length scale representing the thickness of the epilimnion and Ri is the Richardson number of the wind induced flow.

It can be argued that the right hand side of (55) represents a sort of bulk flux Richardson number (this parameter is related to the concept of mixing efficiency as is discussed in the next section), and therefore with arguments similar to those used in the previous section, can be considered as a constant coefficient. Defining:

$$3c_w\ \frac{\rho_1}{\rho_0}\ \frac{A_s}{A_t} - \frac{2\ \Phi}{\rho_0\ A_t\ u_{*s}^3} = c_e \tag{57}$$

and replacing this result in equation (55) gives:

$$\frac{u_e}{u_{*s}} = \frac{c_e}{Ri} \tag{58}$$

Entrainment relationships such as that given by (58) have been proposed in the literature coming from different sources, including experimental and numerical research. It has been argued that the entrainment mechanism is different for a situation where the presence of endwalls of the water basin is not yet noticeable, and the situation where wind set-up has already created streamwise pressure gradients.

To avoid unwanted endwall effects, Kato and Phillips (1969), Kantha et al. (1977) and Deardorff and Willis (1982) carried out experiments in annular tanks to simulate one-dimensional entrainment processes of large horizontal extent. However, channel curvature induces secondary flow that affects the entrainment process (Scranton and Lindberg, 1983). Because of this, Kranenburg (1984) avoided the use of annular tanks, using instead an experimental technique consisting in re-circulating the excess water resulting from wind set-up in a wind flume, thus precluding longitudinal pressure gradients to build up. Experiments that include endwall effects on vertical mixing due to surface shear stress have also been conducted. Kranenburg (1985) carried out experiments in a wind flume, while Monismith (1986), Stevens and Imberger (1996) and Niño et al. (2002) applied the surface shear by means of a conveyor belt.

Kranenburg's (1984) experimental results gave the following entrainment relationship during the fully developed phase of the mixing process, in the zero longitudinal pressure gradient situation:

$$\frac{u_e}{u_{*s}} = \frac{0.6}{(Ri)^{1/2}} \tag{59}$$

This relationship is similar to that obtained by Price (1979) and Thompson (1979), extrapolating Kantha et al.'s (1977) results to zero aspect ratio of their annular flume.

In the case when endwalls effects are present, the entrainment rate is reduced with respect to that of the zero pressure gradient case. Kranenburg (1985) obtained, based on Wu's (1973) and his own experiments, the following entrainment relationship, which was also confirmed later by Monismith (1986) and Niño et al. (2002), through experimental research, and Chu and Soong (1997), through numerical modeling:

$$\frac{u_e}{u_{*s}} = \frac{0.07}{Ri} \tag{60}$$

This result validates the analysis presented in this section and equation (58), giving a value $c_e = 0.07$. However, results by Chu and Soong (1997) and Niño et al. (2002) have indicated that

the length to height ratio of the flow, L/H where L denotes the fetch of the wind and H is the total flow depth, may play an important role on the entrainment process, affecting the value of c_e in (58).

3 Other sources of mixing

It can be shown that the entrainment velocity resulting from penetrative convection, for typical heat fluxes associated to the cooling of lakes and reservoirs, is generally of the same order of magnitude as that resulting from wind mixing, for typical values of wind velocity in lakes and reservoirs. Metalimnion mixing associated to these processes is of an intermittent nature. Strong mixing in this region is rare and associated, mainly, to strong wind events or strong cooling events. In any case, both processes contribute to maintaining a well mixed epilimnion.

The metalimnion, however, can also be subject to other mixing processes. One of them, associated with the breaking of internal gravity waves. Different mechanisms create the conditions for wave steepening and breaking. A recent review of these mechanisms can be found in Staquet and Sommeria (2002). Nonetheless, it is important to recognize the importance of the internal seiching motion set up by the wind. The energy stored in this motion is then transferred to shorter and shorter waves, and then to turbulence and mixing, through the wave breaking mechanisms just noted. Also, the energy contained in relatively short internal waves is radiated towards the boundary where is partially dissipated due to shoaling induced breaking and other mechanisms. These processes energize the benthic boundary layer as is discussed below.

Within the metalimnion, turbulence is affected by buoyancy effects, which creates a rather stable environment. A simple turbulent kinetic energy budget within this region can be expressed as:

$$P + G - \epsilon = 0 \tag{61}$$

where P denotes the production rate of turbulent kinetic energy, G the rate of turbulent kinetic energy used to overcome buoyancy effects, and ϵ is the rate of turbulent kinetic energy dissipation. Dividing (61) by this latter term, yields:

$$\frac{P}{\epsilon} = 1 - \frac{G}{\epsilon} \tag{62}$$

Defining the *mixing efficiency*, γ_{mix}, as:

$$\gamma_{mix} = -\frac{G}{\epsilon} \tag{63}$$

then, from (62):

$$\frac{P}{\epsilon} = 1 + \gamma_{mix} \tag{64}$$

Now, the definitions for the production, P, and buoyancy, G, terms in a system with mean flow velocity $\bar{u}$ in the horizontal direction, with only vertical gradient $\partial\bar{u}/\partial z$, are:

$$P = -\overline{u'w'}\,\frac{\partial \bar{u}}{\partial z} \quad ; \quad G = -\frac{g}{\rho_0}\,\overline{w'\rho'} \tag{65}$$

where $\overline{u'w'}$ and $\overline{w'\rho'}$ represent the horizontal Reynolds shear stress and the vertical turbulent mass flux, respectively. Thus, introducing usual closures in terms of the eddy viscosity, ν_t, and eddy diffusivity, D_t:

$$-\overline{u'w'} = \nu_t \, \frac{\partial \bar{u}}{\partial z} \quad ; \quad -\overline{w'\rho'} = D_t \, \frac{\partial \bar{\rho}}{\partial z} \tag{66}$$

yields:

$$G = \frac{g}{\rho_0} \, D_t \, \frac{\partial \bar{\rho}}{\partial z} = -N^2 \, D_t \tag{67}$$

where, N denotes the buoyancy frequency defined as:

$$N^2 = -\frac{g}{\rho_0} \, \frac{\partial \bar{\rho}}{\partial z} \tag{68}$$

and:

$$P = \nu_t \, (\frac{\partial \bar{u}}{\partial z})^2 \tag{69}$$

Replacing (67) in (63) finally yields:

$$\gamma_{mix} = \frac{N^2 \, D_t}{\epsilon} \tag{70}$$

or:

$$D_t = \gamma_{mix} \, \frac{\epsilon}{N^2} \tag{71}$$

which provides an estimation of the eddy diffusivity in the metalimnion, given measured values of the rate of dissipation, ϵ, and the buoyancy frequency, N, in this region. Equation (71) is known as Osborn (1980) relation. A value of $\gamma_{mix} = 0.15$ is proposed by Wüest and Lorke (2003), which would be consistent with field observations.

Replacing (69) in (64) gives:

$$\nu_t = \frac{(1 + \gamma_{mix}) \, \epsilon}{(\partial \bar{u}/\partial z)^2} \tag{72}$$

which is a less useful result than (71) because it needs the velocity gradient as input, which is always difficult to estimate.

Note that it is easy to show that the mixing efficiency γ_{mix} is related with the concept of flux Richardson number, $R_f = -G/P$, introduced in previous lecture notes:

$$1 + \gamma_{mix} = \frac{1}{1 - R_f} \tag{73}$$

Very little turbulent kinetic energy leaks below the metalimnion, and this region, the hypolimnion, remains quiescent and therefore very stable, almost laminar, except for some turbulent patches and fossil turbulent structures distributed randomly in the water column.

In contrast, the benthic boundary layer (BBL) has much higher levels of turbulent kinetic energy, comparable with those of the epilimnion (Wüest and Lorke, 2003). Mixing in the BBL, is therefore

much more important than that in the hypolimnion. Sources for the turbulent kinetic energy in the BBL come from density currents, triggered by inflows, and large scale internal seiches. In the latter case, the large scale motion created by the internal seiches in the hypolimnion, generates currents with near-bed velocity gradients that are large enough to produce turbulent kinetic energy. Strong mixing and turbulence in the BBL is responsible for energizing mass transfer between the sediments and the water column, and therefore has a major importance in modulating chemical and biological processes that determine water quality within the hypolimnion and the water body as a whole.

Within the BBL, the scaling appropriate for wall bounded flows is valid. This leads to a logarithmic velocity profile. For example, assuming local equilibrium, so production equals dissipation ($P \approx \epsilon$), and also a constant stress layer near the bed, the eddy viscosity can be estimated as:

$$\nu_t = \kappa \, u_{*b} \, z \tag{74}$$

where κ is von Karman's constant, z is the distance from the bed and u_{*b} is the bed shear velocity. Assuming Reynolds analogy, i.e., $\nu_t = D_t$, leads therefore to:

$$D_t = \kappa \, u_{*b} \, z \tag{75}$$

and it is concluded that the eddy diffusivity increases linearly with the distance from the bed, within the wall region of the BBL. The same scaling leads to the following expression for the rate of dissipation of turbulent kinetic energy in the same region:

$$\epsilon = \frac{u_{*b}^3}{\kappa \, z} \tag{76}$$

The flow velocity within the wall region is, therefore, logarithmic:

$$\frac{\bar{u}}{u_{*b}} = \frac{1}{\kappa} \, \ln\left(\frac{z}{z_0}\right) \tag{77}$$

where, z_0 is a length scale appropriate to the type of wall in the BBL: hydraulically smooth or rough. Measurements in the field indicate values of u_{*b} that are larger than expected for a smooth wall. This may indicate that the bottom of lakes and reservoirs are actually rough, not because of sediment size but because of irregular bed relief, possibly related to biological activity (Wüest and Lorke, 2003). Other possible source for the enhanced resistance can be related to the existence of an oscillatory boundary layer, forced by internal seiches (Wüest and Lorke, 2003).

In low forced lakes, ambient turbulence may not be able to mix the BBL. Continuous release of dissolved solids from the sediment (by mineralization and other sediment processes) can stabilize the BBL ($N^2 > 0$) and suppress mixing. In this case, Turner's (1973) ideas can be used to modify the near-bed scaling due to buoyancy effects. According to Turner, in the presence of a buoyancy flux, G, defined as in (67), the near-bed turbulence length scale, $l = \kappa \, z$, typically used in the non-stratified case, should be modified to:

$$\tilde{l} = \frac{l}{\phi_m} = \frac{\kappa \, z}{\phi_m} \tag{78}$$

where ϕ_m is a dimensionless function of a dimensionless distance from the bed: $\phi_m = f(z/L)$, where L denotes the *Monin-Obukov length*, defined as:

$$L = \frac{\rho\, u_{*b}^3}{\kappa\, g\, \overline{w'\rho'}} = -\frac{u_{*b}^3}{\kappa\, G} = \frac{u_{*b}^3}{\kappa\, N^2\, D_t} \tag{79}$$

Turner suggests that a simple expansion truncated at a linear level allows estimation of ϕ_m as:

$$\phi_m \approx 1 + \alpha\, \frac{z}{L} \tag{80}$$

where α is a constant with a value of about 5.

Using the modified length scale, $\tilde{l}$, the near-bed eddy viscosity in the stratified BBL is given by:

$$\nu_t = \frac{\kappa\, z\, u_{*b}}{\phi_m} \tag{81}$$

which leads to the buoyancy affected log-linear velocity profile:

$$\frac{\bar{u}}{u_{*b}} = \frac{1}{\kappa}\, \{\ln(\frac{z}{z_0}) + \alpha\, \frac{z}{L}\} \tag{82}$$

Using (72), (81) and (82), it can be shown that the dissipation rate, affected by buoyancy, in the near-bed region is given by:

$$\epsilon = (\frac{1}{1+\gamma_{mix}})\, \frac{u_{*b}^3}{\kappa\, z}\, \phi_m = (1 - R_f)\, \frac{u_{*b}^3}{\kappa\, z}\, \phi_m \tag{83}$$

However, it can be demonstrated that in the near-bed region, the flux Richardson number is reduced to:

$$R_f = \frac{\nu_t}{\kappa\, L\, u_{*b}} = \frac{z/L}{\phi_m} \tag{84}$$

so replacing this result in (83) yields:

$$\epsilon = (\phi_m - \frac{z}{L})\, \frac{u_{*b}^3}{\kappa\, z} = (1 + (\alpha - 1)\, \frac{z}{L})\, \frac{u_{*b}^3}{\kappa\, z} \tag{85}$$

Neglecting the buoyancy correction and using Osborn relation (71), Wüest and Lorke (2003) maintain that the buoyancy affected eddy diffusivity in the near-bed region of the BBL can be estimated as:

$$D_t = \gamma_{mix}\, \frac{u_{*b}^3}{\kappa\, z\, N^2} \tag{86}$$

It is easy to see from (73) and (84) that γ_{mix} decreases to zero as the bed is approached. This means that buoyancy effects are not important in the very near bed region and that the eddy diffusivity there is then given by (75). This result indicates that the eddy diffusivity first tends to increase away from the bed, governed by (75), up to a distance $z \approx \gamma_{mix}^{1/2}\, u_{*b}/(\kappa\, N)$, obtained by equating equations (75) and (86). Above this elevation, buoyancy effects become important and the eddy diffusivity decreases as z increases, according to (86).

As a final summary of the material presented in the present notes, most of the mixing processes observed in lakes and reservoirs discussed previously are represented schematically in Fig. 5, which was adapted from Fischer et al. (1979).

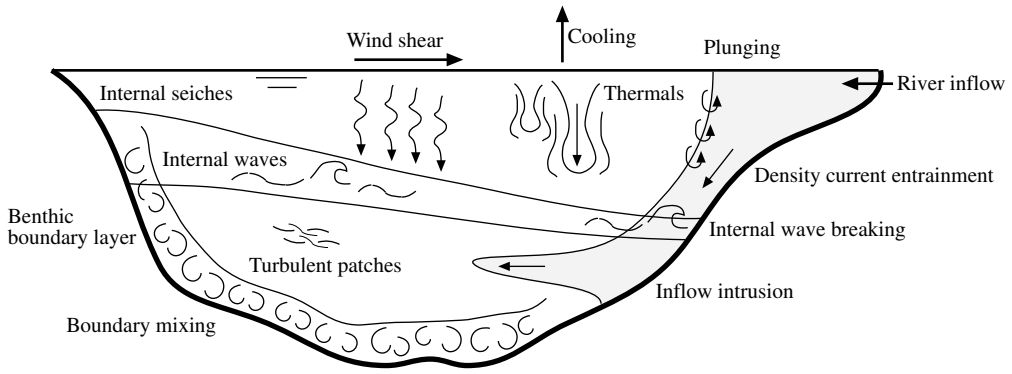

Figure 5: Sources of mixing in lakes and reservoirs. Adapted from Fischer et al. (1979)

4 References

- Chu, C. R. and Soong, C. K. (1997). Numerical simulation of wind-induced entrainment in a stably stratified water basin. J. Hydr. Res., Vol. 35, No. 1, pp. 21-41.
- Deardorff, J. W. and Willis, G. E. (1982). Dependence of mixed-layer entrainment on shear stress and velocity jump. J. Fluid Mech., 115, pp. 123-150.
- Fisher, List, Koh, Imberger and Brooks. (1979). Mixing in Inland and Coastal Waters. Academic Press.
- Kantha, L. H., Phillips, O. M., and Azad, R. S. (1977). On turbulent entrainment at a stable density interface. J. Fluid Mech., 93, pp. 753-768.
- Kato, H. and Phillips, O. M. (1969). On the penetration of a turbulent layer intro stratified fluid. J. Fluid Mech., 37, pp. 643-655.
- Kranenburg, C. (1984). Wind-induced entrainment in a stably stratified fluid. J. Fluid Mech., 145, pp. 253-273.
- Kranenburg, C. (1985). Mixed-layer deepening in lakes after wind setup. J. Hydr. Engrg., Vol. 111, No. 9, pp. 1279-1297.
- Monismith, S. G. (1986). An experimental study of the upwelling response of stratified reservoirs to surface shear stress. J. Fluid Mech., 171, pp. 407-439.
- Niño, Y., Caballero, R., and Reyes, L. (2002). Mixing and interface dynamics in a two-layer stratified fluid due to surface shear stress. J. Hydraul. Res. In Press.
- Osborn, T.R. (1980). Estimates of the local rate of vertical diffusion from dissipation measurements. J. Phys. Oceanogr. 10, pp. 83-89.
- Pedersen. (1986). Environmental Hydraulics. Springer-Verlag.
- Price, J. F. (1979). On the scaling of stress-driven entrainment experiments. J. Fluid Mech., 90, pp. 509-529.

- Scranton, D. R. and Lindberg, W. R. (1983). An experimental study of entraining, stress driven, stratified flow in an annulus. Phys. Fluids, 26, pp. 1198-1205.
- Staquet, C. and Sommeria, J. (2002). Internal gravity waves: from instabilities to turbulence. Annu. Rev. Fluid Mech., 34, pp. 559-593.
- Stevens, C. and Imberger, J. (1996). The initial response of a stratified lake to a surface shear stress. J. Fluid Mech., 312, pp. 39-66.
- Thompson, R. O. R. Y. (1979). A reinterpretation of the entrainment process in some laboratory experiments. Dyn. Atmos. Oceans, 4, pp. 45-55.
- Turner, J.S. (1973). Buoyancy Effects in Fluids. Cambridge University Press.
- Wüest, A. and Lorke, A. (2003). Small-scale hydrodynamics in lakes. Annu. Rev. Fluid Mech., 35, pp. 375-412.